LFV, LNV processes and new physics at the same-sign muon colliders

***Jin-Lei. Yang**, Chao-Hsi. Chang and Tai-Fu. Feng, Chin. Phys. C 48 (2024) 4, 043101*

Hebei University   Jin-Lei Yang

PKU   2024/04/20

Content

1 Introduction

- **The motivation of studying the LFV and LNV processes at the same-sign muon colliders**

LFV： $\mu^{\pm}\mu^{\pm} \rightarrow \tau^{\pm}\tau^{\pm}, \mu^{\pm}\mu^{\pm} \rightarrow e^{\pm}e^{\pm}$

LNV： $\mu^{\pm}\mu^{\pm} \rightarrow W^{\pm}W^{\pm}$

1, the LFV processes do not depend on the large flavor mixing parameters, for example

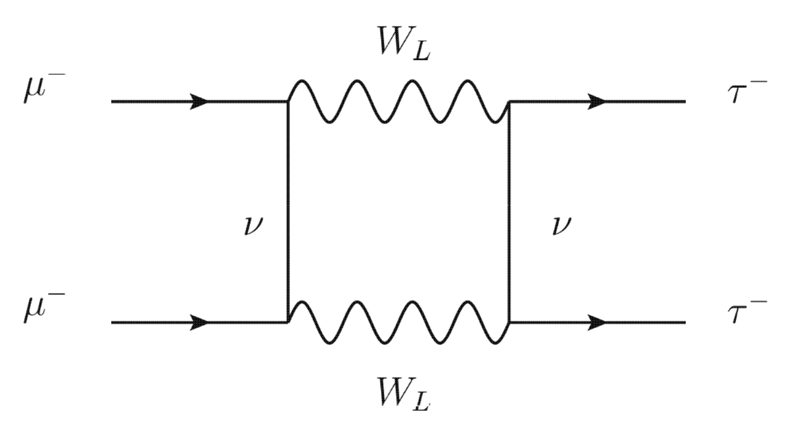

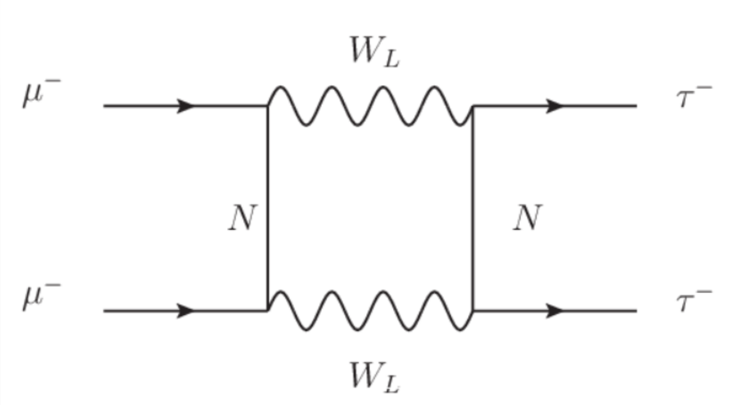

1 Introduction

2 , strict constraints from the nuclear 0ν2β decays

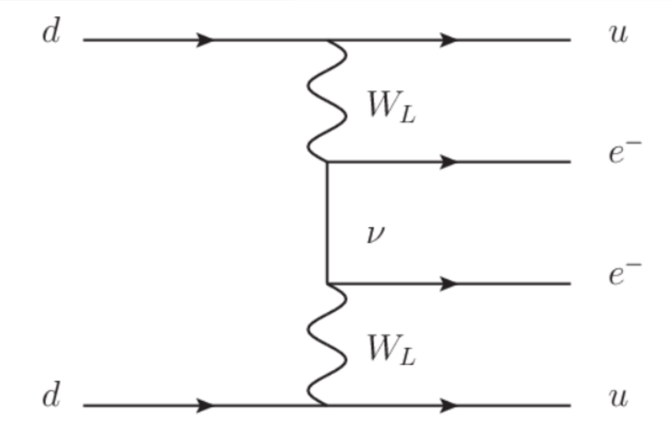

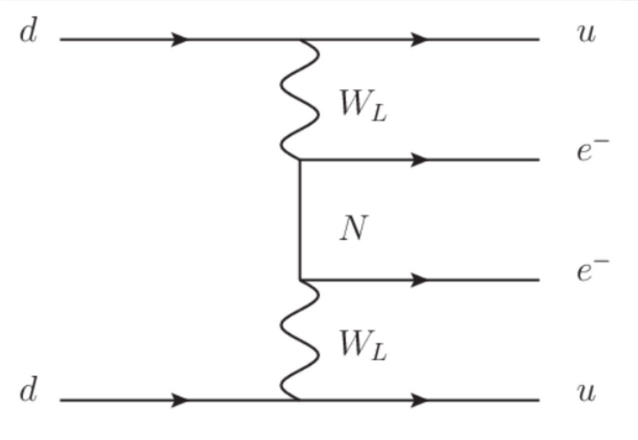

3, the muon collider can reach higher collider energy comparted with the electron collider

$$\frac{m_\mu}{m_e} \approx 207$$

1 Introduction

Possible contributions in NP

Majorana neutrinos — W_L, W_R → contribute to the LFV processes at the one-loop level; contribute to the LNV processes at the tree level

Doubly charged Higgs → contribute to the LFV and LNV processes at the tree level

The meaning of observing LFV and LNV at the same-sign muon collider

1, providing definite evidences of NP beyond the SM

2, identifying the nature of neutrinos

3, searching new particle: doubly charged Higgs

2 Theoretical calculation

Types of NP

	Particle contents contribute to LFV and LNV in NP
Type I new physics (**TI-NP**)	Majorana neutrinos； W_L
Type II new physics (**TII-NP**)	Majorana neutrinos； W_L； W_R
Type III new physics (**TIII-NP**)	Majorana neutrinos； W_L； W_R； doubly charged Higgs

representative NP models

TI-NP： B-LSSM, NMSSM, …

TII-NP： LRSM without triplet

TIII-NP： LRSM, LRSSM,…

The needed Lagrangian for **TI-NP** can be extracted from B-LSSM, and for **TII-NP**, **TIII-NP** can be extracted from LRSM.

2 Theoretical calculation

Majorana neutrinos in the B-LSSM

New $U(1)_{B-L}$, three right-handed neutrinos and two scalar singlets are introduced in the B-LSSM, then the tiny neutrino masses can be obtained by the Type-I seesaw mechanism

$$\begin{pmatrix} 0 & M_D^T \\ M_D & M_R \end{pmatrix}$$

The mass matrix above can be diagonalized by a unitary matrix U_ν

$$U_\nu^T \begin{pmatrix} 0 & M_D^T \\ M_D & M_R \end{pmatrix} U_\nu = \begin{pmatrix} \hat{m}_\nu & 0 \\ 0 & \hat{M}_N \end{pmatrix}$$

where $\hat{m}_\nu = \mathrm{diag}\left(m_{\nu_1}, m_{\nu_2}, m_{\nu_3}\right)$, $\hat{m}_N = \mathrm{diag}\left(m_{N_1}, m_{N_2}, m_{N_3}\right)$. The unitary matrix U_ν reads

$$U_\nu = \begin{pmatrix} U & S \\ T & V \end{pmatrix}$$

2 Theoretical calculation

The Lagrangian involving leptons and W boson in the B-LSSM

$$\mathcal{L}_W^{\mathrm{BL}} = \frac{ig_2}{\sqrt{2}} \sum_{j=1}^{3} \left[U_{ij} \bar{e}_i \gamma^\mu P_L \nu_j W_{L,\mu} + S_{ij} \bar{e}_i \gamma^\mu P_L N_j W_{L,\mu} + h.c. \right]$$

The relevant couplings of leptons and Goldstones are

$$\mathcal{L}_G^{\mathrm{BL}} = \frac{ig_2}{\sqrt{2} M_{W_L}} \sum_{j=1}^{3} \Big\{ \bar{e}_i \left[\left(M_D^{\dagger} \cdot T^* \right)_{ij} P_R - (\hat{m}_l \cdot U)_{ij} P_L \right] \nu_j G_L +$$

$$\bar{e}_i \left[\left(M_D^{\dagger} \cdot V^* \right)_{ij} P_R - (\hat{m}_l \cdot S)_{ij} P_L \right] N_j G_L + h.c. \Big\}$$

We can define $S_i^2 = \sum_{j=1}^{3} |S_{ij}^2| (i = e, \mu, \tau)$ to describe the strength of light-heavy neutrino mixings.

2 Theoretical calculation

Majorana neutrinos in the LRSM

New $SU(2)_R$, three right-handed neutrinos and two scalar trilets are introduced in the LRSM, then the tiny neutrino masses can be obtained by the Type-I+II seesaw mechanism

$$\begin{pmatrix} M_L & M_D^T \\ M_D & M_R \end{pmatrix}$$

The mass matrix can also be diagonalized by the unitary matrix U_ν. The W boson mass matrix in the LRSM can be written as

$$\frac{g_2^2}{4}(W_L, W_R)\begin{pmatrix} v_1^2+v_2^2+2v_L^2 & 2v_1v_2 \\ 2v_1v_2 & v_1^2+v_2^2+2v_R^2 \end{pmatrix}\begin{pmatrix} W_L \\ W_R \end{pmatrix}$$

The physical masses of the two W bosons are

$$M_{W_1} \approx \frac{g_2}{2}\left(v_1^2+v_2^2\right)^{\frac{1}{2}}, \qquad M_{W_2} \approx \frac{g_2}{\sqrt{2}} v_R$$

2 Theoretical calculation

The mass eigenstates W_1, W_2 are related to the gauge eigenstates W_L, W_R by

$$\begin{pmatrix} W_1 \\ W_2 \end{pmatrix} = \begin{pmatrix} \cos\zeta & \sin\zeta \\ -\sin\zeta & \cos\zeta \end{pmatrix} \begin{pmatrix} W_L \\ W_R \end{pmatrix}$$

Where $\tan\zeta = \frac{2v_1 v_2}{(v_R^2 - v_L^2)}$. The Lagrangian involving leptons and W boson in the LRSM

$$\mathcal{L}_W^{\mathrm{LR}} = \frac{i g_2}{\sqrt{2}} \sum_{j=1}^{3} \Big[\bar{e}_i \big(\cos\zeta\, U_{ij} \gamma^\mu P_L + \sin\zeta\, T_{ij}^* \gamma^\mu P_R \big) \nu_j W_{1,\mu} + \bar{e}_i \big(\cos\zeta\, T_{ij}^* \gamma^\mu P_R - \sin\zeta\, U_{ij} \gamma^\mu P_L \big) \nu_j W_{2,\mu}$$
$$+ \bar{e}_i \big(\cos\zeta\, S_{ij} \gamma^\mu P_L + \sin\zeta\, V_{ij}^* \gamma^\mu P_R \big) N_j W_{1,\mu} + \bar{e}_i \big(\cos\zeta\, V_{ij}^* \gamma^\mu P_R - \sin\zeta\, S_{ij} \gamma^\mu P_L \big) N_j W_{2,\mu} + h.c. \Big]$$

The relevant couplings of leptons and Goldstones in the LRSM are

$$\mathcal{L}_G^{\mathrm{LR}} = \frac{i g_2}{\sqrt{2} M_{W_L}} \sum_{j=1}^{3} \Big\{ \bar{e}_i \big[\lambda_{1,ij} P_L + \lambda_{2,ij} P_R \big] \nu_j G_L + \bar{e}_i \big[\lambda_{3,ij} P_L + \lambda_{4,ij} P_R \big] N_j G_L$$
$$+ \bar{e}_i \big(\lambda_{5,ij} P_L \big) \nu_j G_R + \bar{e}_i \big(\lambda_{6,ij} P_L \big) N_j G_R + h.c. \Big\}$$

where $\lambda_1 = -m_l^\dagger \cdot U,\ \lambda_2 = \widehat{M}_D^\dagger \cdot T^*,\ \lambda_3 = -m_l^\dagger \cdot S,\ \lambda_4 = \widehat{M}_D^\dagger \cdot V^*,\ \ \lambda_5 = \frac{M_{W_1}}{M_{W_2}} M_R^\dagger \cdot T,\ \ \lambda_6 = \frac{M_{W_1}}{M_{W_2}} M_R^\dagger \cdot V^*$

2 Theoretical calculation

The Lagrangian involving leptons and doubly charged Higgs in the LRSM

$$\mathcal{L}_{\Delta ll}^{\mathrm{LR}} = i2Y_{L,ij}\bar{e}P_L e_j^C \Delta_L^{--} + i2Y_{R,ij}\bar{e}P_R e_j^C \Delta_R^{--} + h.c.$$

The Lagrangian involving W bosons and doubly charged Higgs in the LRSM

$$\mathcal{L}_{\Delta WW}^{\mathrm{LR}} = i\sqrt{2}g_2^2 v_L \Delta_L^{--} W_1^{\mu+} W_{1\mu}^{+} + i\sqrt{2}g_2^2 v_L \sin\zeta\, \Delta_L^{--} W_1^{\mu+} W_{2\mu}^{+}$$
$$+ i\sqrt{2}g_2^2 v_R \sin\zeta\, \Delta_R^{--} W_1^{\mu+} W_{2\mu}^{+} + i\sqrt{2}g_2^2 v_R \Delta_R^{--} W_2^{\mu+} W_{2\mu}^{+} + h.c.$$

- **The relevant Lagrangian for TI-NP, TII-NP and TIII-NP**

TI-NP： $\mathcal{L}_W^{\mathrm{BL}}$、$\mathcal{L}_G^{\mathrm{BL}}$

TII-NP： $\mathcal{L}_W^{\mathrm{LR}}$、$\mathcal{L}_G^{\mathrm{LR}}$

TIII-NP： $\mathcal{L}_W^{\mathrm{LR}}$、$\mathcal{L}_G^{\mathrm{LR}}$、$\mathcal{L}_{\Delta ll}^{\mathrm{LR}}$、$\mathcal{L}_{\Delta WW}^{\mathrm{LR}}$

2 Theoretical calculation

- **The leading order contributions from Majorana neutrinos and doubly charged Higgs to the LFV processes**

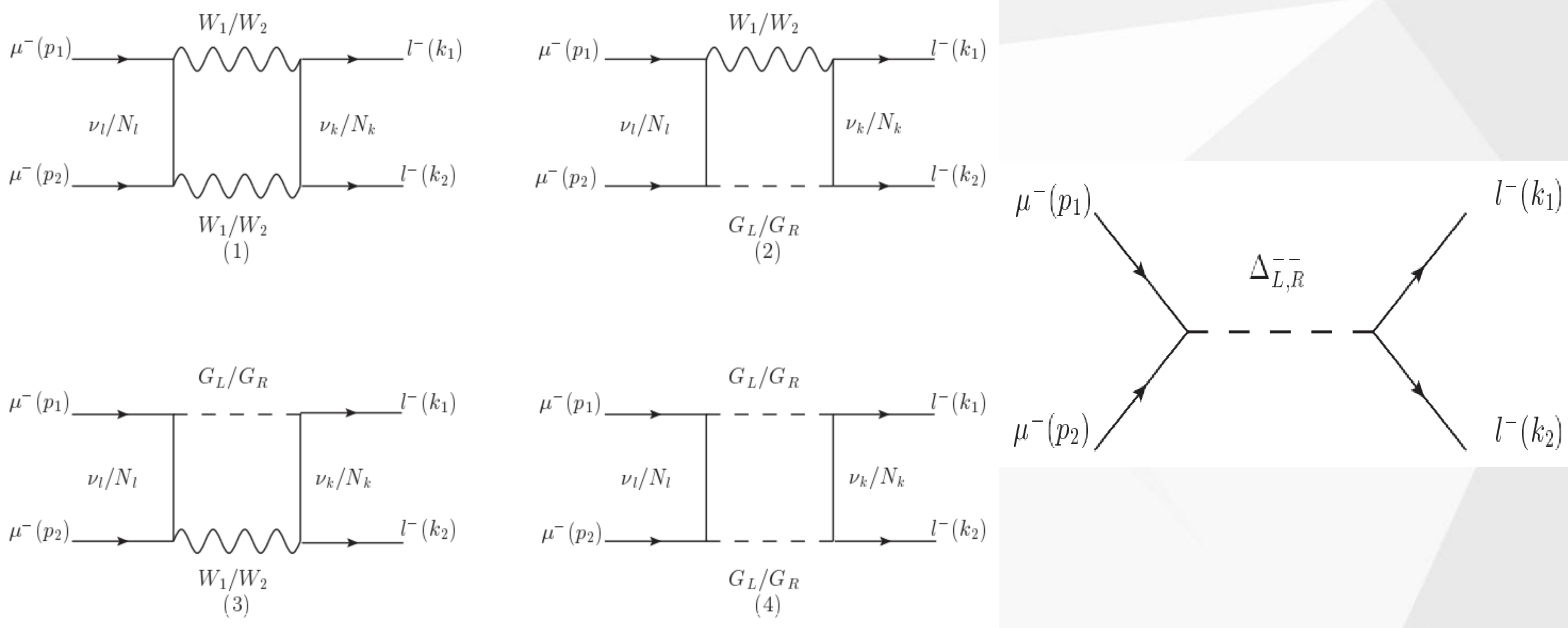

Fig. 1. The leading order contributions from Majorana neutrinos (left) and doubly charged Higgs (right) to the LFV processes in the Feynman gauge.

2 Theoretical calculation

The amplitude can be simplified by neglecting charged lepton masses

$$\mathcal{M}\left(\mu^{\pm}\mu^{\pm} \to l^{\pm}l^{\pm}\right) = \frac{i}{16\pi^2}\sum_{i=1}^{7}\sum_{X,Y=L,R} C_i^{XY}\mathcal{O}_i^{XY}$$

where

$$\begin{aligned}
\mathcal{O}_1^{XY} &= \bar{u}(k_1)\gamma_\mu P_X u^c(k_2)\overline{u^c}(p_2)\gamma^\mu P_Y u(p_1)\\
\mathcal{O}_2^{XY} &= \bar{u}(k_1)p_1^\alpha\gamma_\alpha P_X u^c(k_2)\overline{u^c}(p_2)k_1^\beta\gamma_\beta P_Y u(p_1)\\
\mathcal{O}_3^{XY} &= \bar{u}(k_1)P_X u^c(k_2)\overline{u^c}(p_2)P_Y u(p_1)\\
\mathcal{O}_4^{XY} &= \bar{u}(k_1)\gamma_\mu P_X u^c(k_2)\overline{u^c}(p_2)\gamma^\mu k_1^\beta\gamma_\beta P_Y u(p_1)\\
\mathcal{O}_5^{XY} &= \bar{u}(k_1)\gamma_\mu p_1^\alpha\gamma_\alpha P_X u^c(k_2)\overline{u^c}(p_2)\gamma^\mu P_Y u(p_1)\\
\mathcal{O}_6^{XY} &= \bar{u}(k_1)P_X u^c(k_2)\overline{u^c}(p_2)k_1^\beta\gamma_\beta P_Y u(p_1)\\
\mathcal{O}_7^{XY} &= \bar{u}(k_1)p_1^\alpha\gamma_\alpha P_X u^c(k_2)\overline{u^c}(p_2)P_Y u(p_1)
\end{aligned}$$

The coefficients contributed by doubly charged Higgs can be read directly

$$C_3^{LR}\left(\Delta_L^{\pm\pm}\right) = \frac{4Y_{L,22}Y_{L,jj}}{(p_1+p_2)^2 - M_{\Delta_L^{\pm\pm}}^2 + iM_{\Delta_L^{\pm\pm}}\Gamma_{\Delta_L^{\pm\pm}}}, \quad C_3^{RL}\left(\Delta_R^{\pm\pm}\right) = \frac{4Y_{R,22}Y_{R,jj}}{(p_1+p_2)^2 - M_{\Delta_R^{\pm\pm}}^2 + iM_{\Delta_R^{\pm\pm}}\Gamma_{\Delta_R^{\pm\pm}}}$$

2 Theoretical calculation

The dominant decay channels of doubly charged Higgs：

$$\Delta_L^{\pm\pm} \to l^{\pm}l^{\pm}, W_1^{\pm}W_1^{\pm}$$
$$\Delta_R^{\pm\pm} \to l^{\pm}l^{\pm}, W_2^{\pm}W_2^{\pm(*)}, W_2^{\pm}W_2^{\pm}$$

- **The leading order contributions from Majorana neutrinos and doubly charged Higgs to the LNV processes**

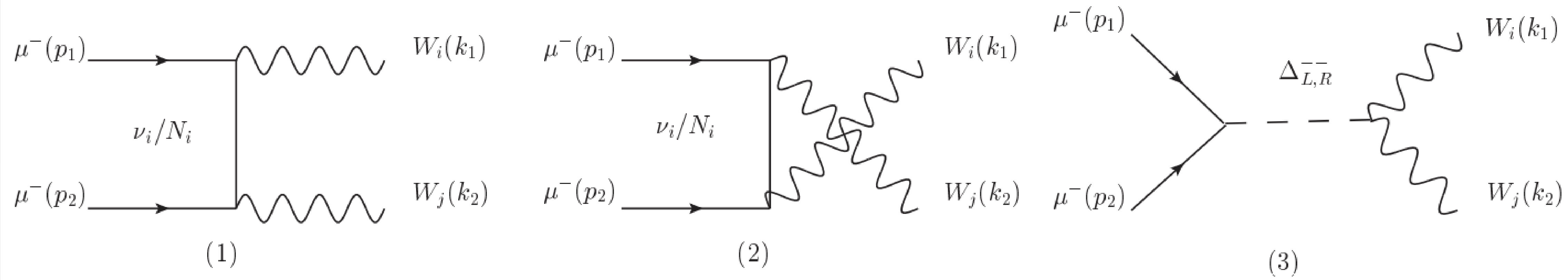

Fig. 2. The leading order contributions from Majorana neutrinos (1, 2) and doubly charged Higgs (3) to the LNV processes.

2 Theoretical calculation

Summing up the fermions' spin and gauge bosons' polarizations, the squared amplitude for the LNV processes can be obtained

$$\left|\mathcal{M}\left(\mu^\pm\mu^\pm \to W_1^\pm W_1^\pm\right)\right|^2 \approx \frac{g_2^4}{M_{W_1}^4}\Big\{\left(\left|C_t^{11}\right|^2 + \left|C_u^{11}\right|^2\right) M_{W_1}^2 (2p_1\cdot k_1 p_1\cdot k_2 + M_{W_1}^2 p_1\cdot p_2/2) + 2\left|C_t^{11}\right|^2 k_1\cdot k_2 (p_1\cdot k_1)^2 + 2\left|C_u^{11}\right|^2 k_1\cdot k_2 (p_1\cdot k_2)^2 + \mathcal{R}\left(C_t^{11} C_u^{11*}\right)[2p_1\cdot p_2 (k_1\cdot k_2)^2 + M_{W_1}^2\left(3M_{W_1}^2 p_1\cdot p_2 - 4p_1\cdot k_1 p_1\cdot k_2\right) - 2k_1\cdot k_2((p_1\cdot k_1)^2 + (p_1\cdot k_2)^2)\Big\}$$

$$\left|\mathcal{M}\left(\mu^\pm\mu^\pm \to W_1^\pm W_2^\pm\right)\right|^2 \approx \frac{g_2^4}{2M_{W_1}^2 M_{W_2}^2}\{\left|C_t^{12}\right|^2 [4M_{W_1}^2 M_{W_2}^2 p_1\cdot k_1 (p_2\cdot k_1 - p_1\cdot p_2) + 8M_{W_1}^2 p_1\cdot k_1 p_2\cdot k_2 (k_1\cdot k_2 - p_1\cdot k_2) - M_{W_1}^4 (M_{W_2}^2 p_1\cdot p_2 + 2p_2\cdot k_2 p_1\cdot k_2) + 4(p_1\cdot k_1)^2 (M_{W_2}^2 p_1\cdot p_2 + 2p_2\cdot k_2 p_1\cdot k_2)] + \left|C_u^{12}\right|^2 [4M_{W_1}^2 M_{W_2}^2 p_1\cdot k_2 (p_2\cdot k_2 - p_1\cdot p_2) + 8M_{W_2}^2 p_1\cdot k_2 p_2\cdot k_1 (k_1\cdot k_2 - p_1\cdot k_1) - M_{W_2}^4 (M_{W_1}^2 p_1\cdot p_2 + 2p_2\cdot k_1 p_1\cdot k_1) + 4(p_1\cdot k_2)^2 (M_{W_1}^2 p_1\cdot p_2 + 2p_2\cdot k_1 p_1\cdot k_1)]\}$$

2 Theoretical calculation

$$\left|\mathcal{M}\left(\mu^{\pm}\mu^{\pm}\to W_2^{\pm}W_2^{\pm}\right)\right|^2 \approx \frac{g_2^4}{M_{W_1}^4}\Big\{\left(\left|C_t^{22}\right|^2+\left|C_u^{22}\right|^2\right)M_{W_2}^2(2p_1\cdot k_1 p_1\cdot k_2 +$$

$$M_{W_2}^2 p_1\cdot p_2/2)+2\left|C_t^{22}\right|^2 k_1\cdot k_2(p_1\cdot k_1)^2+2\left|C_u^{11}\right|^2 k_1\cdot k_2(p_1\cdot k_2)^2 +$$

$$\mathcal{R}\left(C_t^{22}C_u^{22*}\right)[2p_1\cdot p_2(k_1\cdot k_2)^2+M_{W_2}^2\left(3M_{W_2}^2 p_1\cdot p_2-4p_1\cdot k_1 p_1\cdot k_2\right)-$$

$$2k_1\cdot k_2((p_1\cdot k_1)^2+(p_1\cdot k_2)^2)\Big\}$$

where

$$C_t^{11}=\cos^2\zeta\left(S_{2j}\right)^2\frac{M_{N_j}}{t-M_{N_j}^2}+\frac{2\sqrt{2}Y_{L,22}v_L}{s-M_{\Delta_L}^2+i\Gamma_{\Delta_L}M_{\Delta_L}}$$

$$C_u^{11}=\cos^2\zeta\left(S_{2j}\right)^2\frac{M_{N_j}}{u-M_{N_j}^2}+\frac{2\sqrt{2}Y_{L,22}v_L}{s-M_{\Delta_L}^2+i\Gamma_{\Delta_L}M_{\Delta_L}}$$

$$C_t^{12}=\cos^2\zeta\left(\frac{T_{2j}^*U_{2j}}{t-m_{\nu_j}^2}+\frac{V_{2j}^*S_{2j}}{t-M_{N_j}^2}\right)$$

$$C_u^{12}=\cos^2\zeta\left(\frac{T_{2j}^*U_{2j}}{u-m_{\nu_j}^2}+\frac{V_{2j}^*S_{2j}}{u-M_{N_j}^2}\right)$$

2 Theoretical calculation

$$C_t^{22} = \cos^2\zeta\left(V_{2j}^*\right)^2 \frac{M_{N_j}}{t - M_{N_j}^2} + \frac{2\sqrt{2}Y_{R,22}v_R}{s - M_{\Delta_R}^2 + i\Gamma_{\Delta_R}M_{\Delta_R}}$$

$$C_u^{22} = \cos^2\zeta\left(V_{2j}^*\right)^2 \frac{M_{N_j}}{u - M_{N_j}^2} + \frac{2\sqrt{2}Y_{R,22}v_R}{s - M_{\Delta_R}^2 + i\Gamma_{\Delta_R}M_{\Delta_R}}$$

$\left|\mathcal{M}\left(\mu^\pm\mu^\pm \to W_1^\pm W_1^\pm\right)\right|^2$ in **TI-NP** and **TII-NP** can be obtained by setting $Y_{L,22} = 0$; $\left|\mathcal{M}\left(\mu^\pm\mu^\pm \to W_2^\pm W_2^\pm\right)\right|^2$ in **TI-NP** can be obtained by setting $Y_{R,22} = 0$. The results of $\sigma\left(\mu^\pm\mu^\pm \to W_1^\pm W_1^\pm\right)$ in **TI-NP** and **TII-NP** are similar; The results of $\sigma\left(\mu^\pm\mu^\pm \to W_1^\pm W_2^\pm\right)$ in **TII-NP** and **TIII-NP** are similar.

3 Numerical results

Experimental constraints

For simplicity, the mass matrix of heavy neutrinos is assumed to be diagonal, the Yukawa coupling of charged leptons and doubly charged Higgs is assumed to be diagonal $Y_L = \mathrm{diag}\left(Y_{ee}, Y_{\mu\mu}, Y_{\tau\tau}\right)$. Considering the sensitivity of future HL-LHC, we take

$$S_\mu^2 \leq 0.01, \quad S_\tau^2 \leq 0.01$$

Y_{ee} and S_e^2 suffer strict constraints from the nuclear 0ν2β decays experimentally,

$$Y_{ee} < 0.04, \quad S_e^2 \leq 10^{-5}$$

The experimental constraints on the right-handed W boson, doubly charged Higgs and neutrino masses

$$M_{W_2} > 4.8\ \mathrm{TeV}, \quad M_{\Delta_L^{\pm\pm}} > 0.8\ \mathrm{TeV}, \quad M_{\Delta_R^{\pm\pm}} > 0.65\ \mathrm{TeV}, \quad \sum_{i=1}^{3} m_{\nu_i} < 0.12\ \mathrm{eV}$$

3 Numerical results

Numerical results for the LFV processes

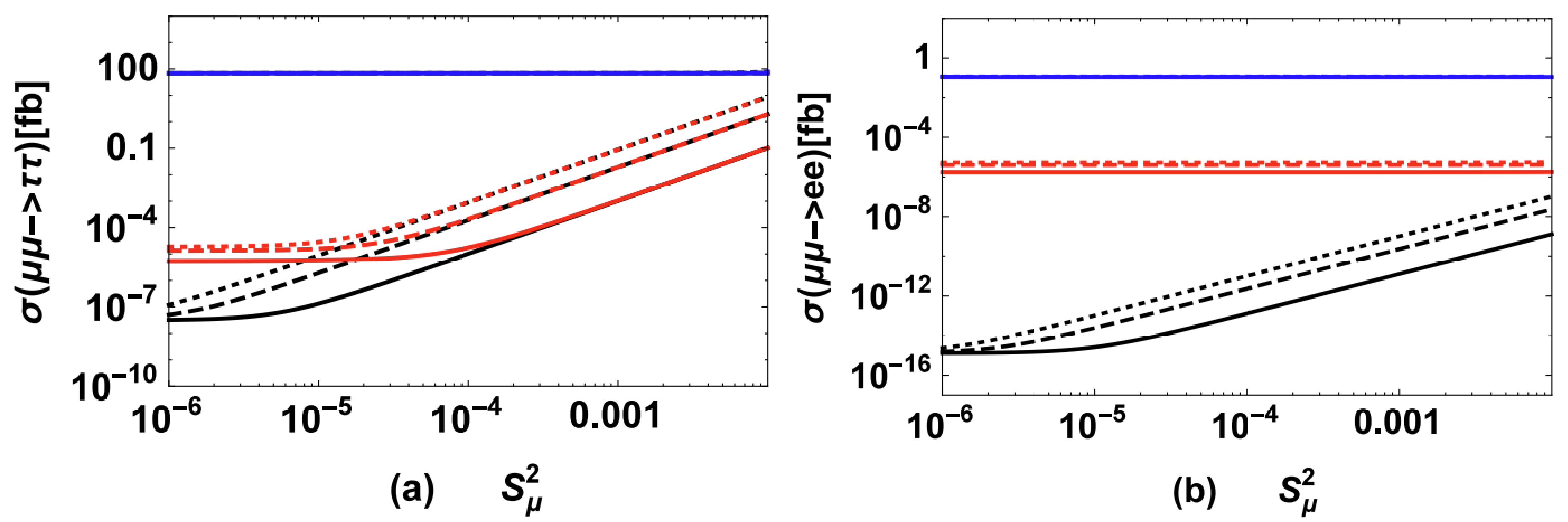

Fig. 3. Taking $M_{N_1} = 1.0$ TeV,$M_{N_3} = 3.0$ TeV,$S_e^2 = 10^{-5}$,$S_\tau^2 = 0.01$ and $\sqrt{s} = 5$ TeV, $\sigma(\mu^\pm\mu^\pm \to l^\pm l^\pm)$ versus S_μ^2 are plotted, where (a) for $l = \tau$, (b) for $l =$ e. The solid, dashed and dotted curves denote the results for $M_{N_2} = 1.0, 2.0, 3.0$ TeV. The black curves denotes the results in **TI-NP**, the red curves denotes the results in **TII-NP** with $M_{W_2} = 5$ TeV, the blue curves denotes the results in **TIII-NP** with $M_{W_2} = 5.0$ TeV、$M_{\Delta^{\pm\pm}} = 3.0$ TeV, $Y_{ee} = 0.04, Y_{\mu\mu} = 1.0, Y_{\tau\tau} = 1.0$.

3 Numerical results

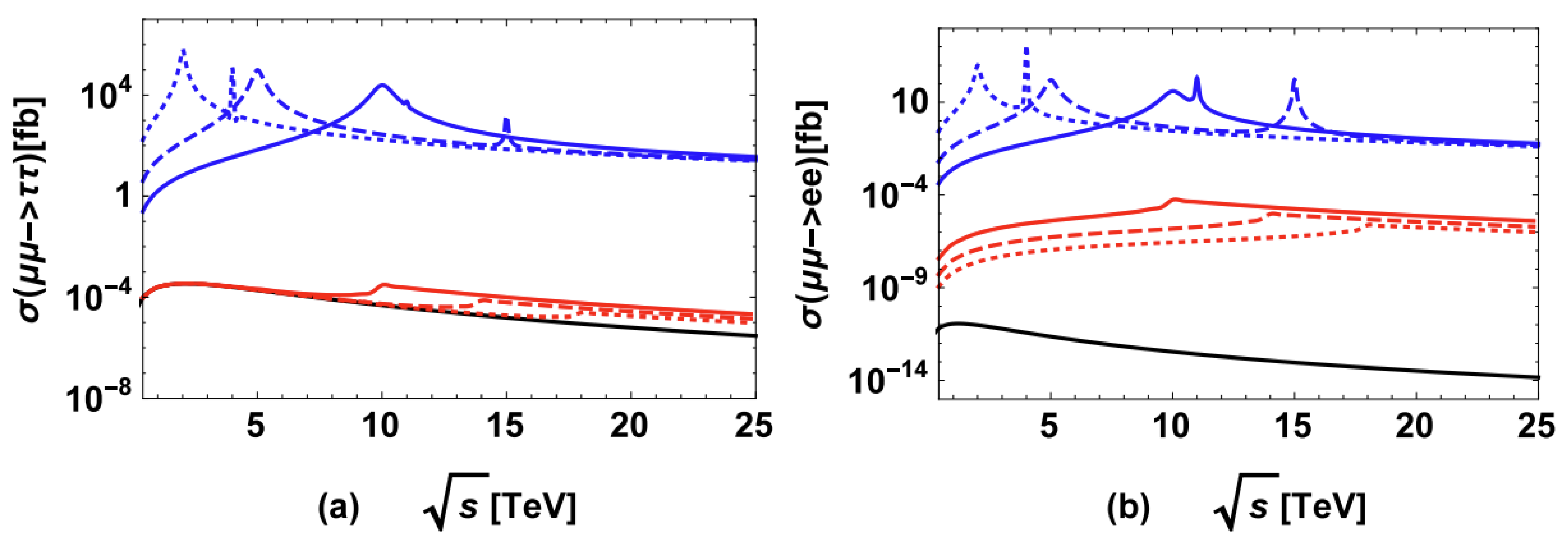

Fig. 4. Taking $M_{N_1} = 1.0$ TeV, $M_{N_2} = 2.0$ TeV, $M_{N_3} = 3.0$ TeV, $S_e^2 = 10^{-5}$, $S_\mu^2 = 10^{-4}$ and $S_\tau^2 = 0.01$, $\sigma(\mu^\pm\mu^\pm \to l^\pm l^\pm)$ versus $\sqrt{s}$ are plotted, where (a) for $l = \tau$, (b) for $l =$ e. The black curves denotes the results in **TI-NP** . The red solid, dashed, dotted curves denote the results in **TII-NP** with $M_{W_2} = 5$ TeV for $M_{W_2} = 5, 7, 9$ TeV respectively. The blue curves denote the results in **TIII-NP** with $M_{W_2} = 5.0$ TeV, $Y_{ee} = 0.04$, $Y_{\mu\mu} = 1.0$, $Y_{\tau\tau} = 1.0$, where the solid curves denote the results for $M_{\Delta_L^{\pm\pm}} = 10.0$ TeV, $M_{\Delta_R^{\pm\pm}} = 11.0$ TeV, the dashed curves denote the results for $M_{\Delta_L^{\pm\pm}} = 5.0$ TeV, $M_{\Delta_R^{\pm\pm}} = 15.0$ TeV , the dotted curves denote the results for $M_{\Delta_L^{\pm\pm}} = 2.0$ TeV, $M_{\Delta_R^{\pm\pm}} = 4.0$ TeV.

3 Numerical results

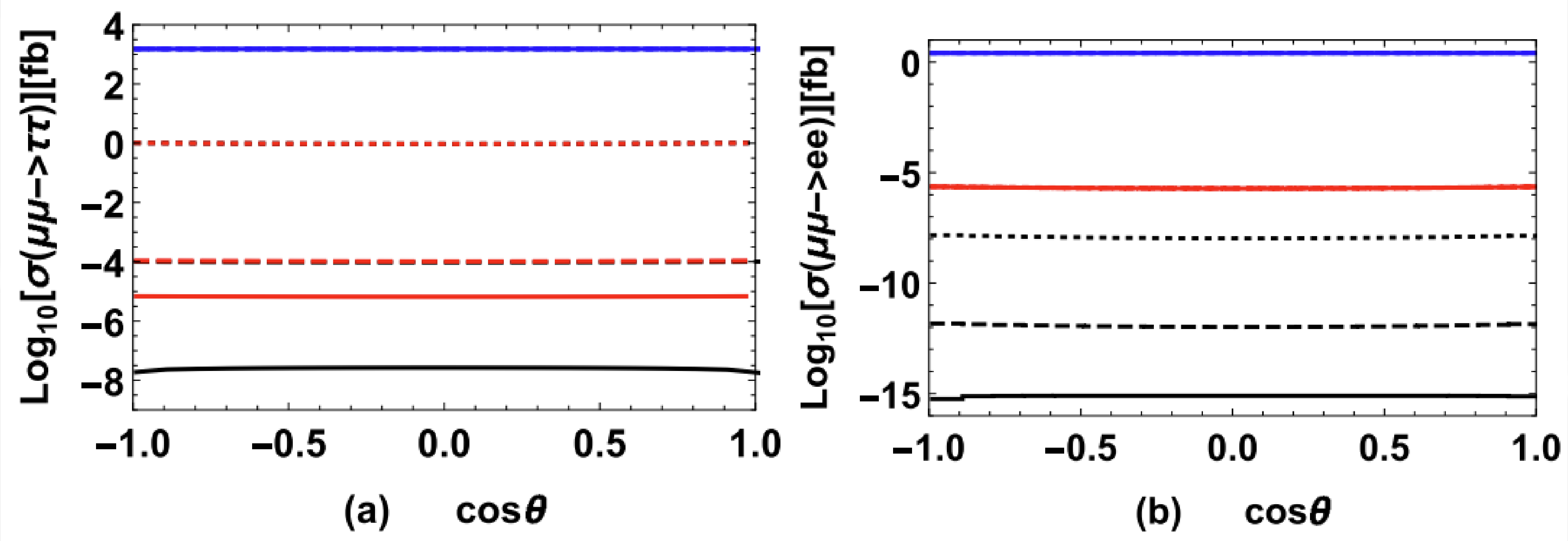

Fig. 5. $M_{N_1}=1.0$ TeV, $M_{N_2}=2.0$ TeV, $M_{N_3}=3.0$ TeV, $S_e^2=10^{-5}$, $S_\tau^2=0.01$ and $\sqrt{s}=5.0$ TeV, the angle distributions of the processes $\mu^\pm\mu^\pm \to l^\pm l^\pm$ are plotted, where (a) for $l=\tau$, (b) for $l=$ e. The solid, dashed and dotted curves denote the results for $S_\mu^2=10^{-6}$、10^{-4}、10^{-2} respectively. The black curves denotes the results in **TI-NP**, the red curves denotes the results in **TII-NP** with $M_{W_2}=5.0$ TeV, the blue curves denotes the results in **TIII-NP** with $M_{W_2}=5.0$TeV, $M_{\Delta_L^{\pm\pm}}=M_{\Delta_R^{\pm\pm}}=3.0$TeV, $Y_{ee}=0.04$, $Y_{\mu\mu}=1.0$ and $Y_{\tau\tau}=1.0$.

3 Numerical results

Numerical results for the LNV processes

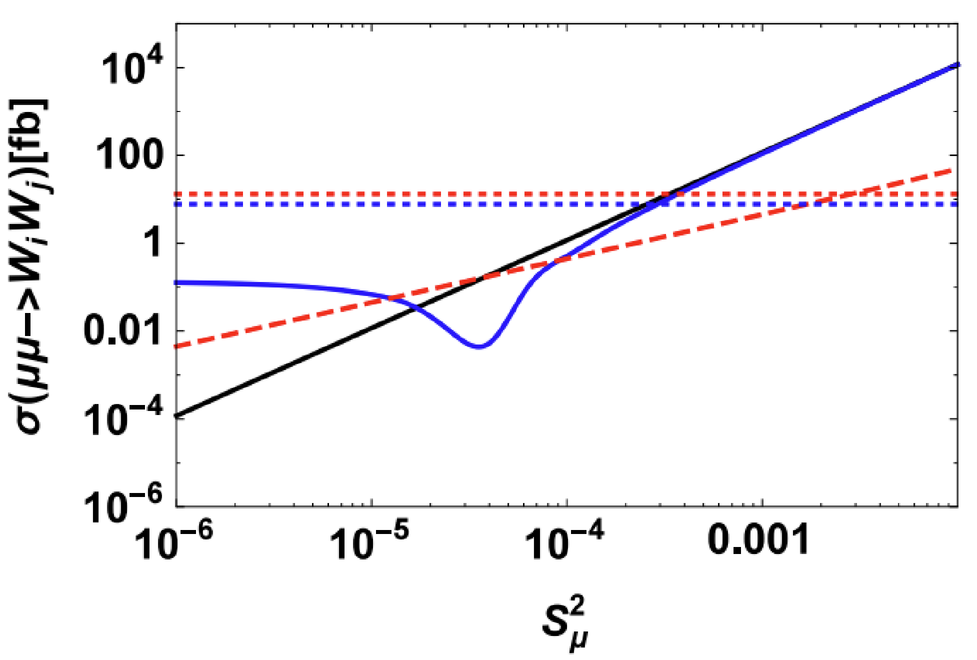

Fig. 6. Taking $M_{N_2} = 2.0\text{TeV}, \sqrt{s} = 15.0$ TeV, $\sigma\left(\mu^\pm\mu^\pm \to W_i^\pm W_j^\pm\right)$ versus S_μ^2 are plotted, where the black solid curve denotes the results in **TI-NP** for $W_iW_j = W_1W_1$, the red dashed and red dotted curves denote the results in **TII-NP** with $M_{W_2} = 5.0$ TeV for $W_iW_j = W_1W_2$ and $W_iW_j = W_2W_2$ respectively, the blue solid and blue dotted curves denote the results in **TIII-NP** with $M_{W_2} = 5.0$ TeV, $M_{\Delta_L^{\pm\pm}} = 10.0$ TeV, $M_{\Delta_R^{\pm\pm}} = 11.0$ TeV, $Y_{\mu\mu} = 1.0$ for $W_iW_j = W_1W_1$ and $W_iW_j = W_2W_2$ respectively.

3 Numerical results

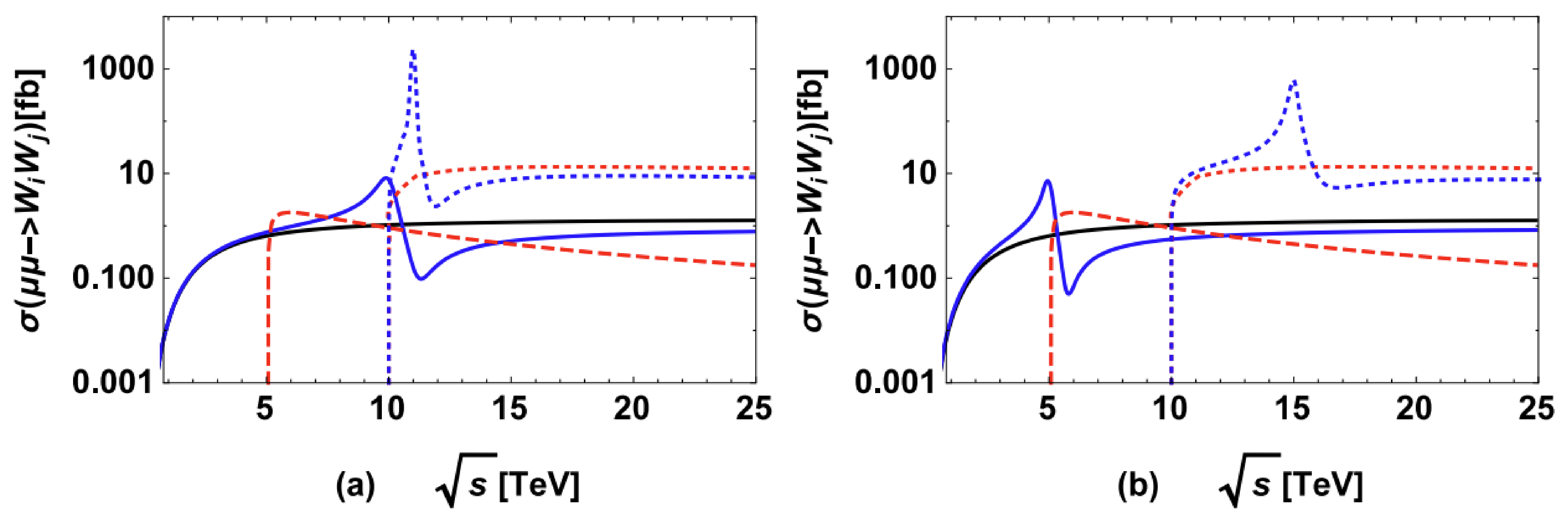

Fig. 7. Taking $M_{N_2} = 2.0$ TeV, $S_\mu^2 = 10^{-4}$, $\sigma\left(\mu^\pm\mu^\pm \to W_i^\pm W_j^\pm\right)$ versus $\sqrt{s}$ are plotted, where the solid, dashed, dotted curves denote $W_iW_j = W_1W_1$, $W_1W_j = W_1W_2$, $W_1W_j = W_2W_2$ respectively. The black curves denotes the results in **TI-NP**. The red curves denotes the results in **TII-NP** with $M_{W_2} = 5.0$ TeV. The blue curves denotes the results in **TIII-NP** with $M_{W_2} = 5.0$ TeV, $Y_{\mu\mu} = 1.0$, where (a) for $M_{\Delta_L^{\pm\pm}} = 10.0$ TeV, $M_{\Delta_R^{\pm\pm}} = 11.0$ TeV and (b) for $M_{\Delta_L^{\pm\pm}} = 5.0$ TeV, $M_{\Delta_R^{\pm\pm}} = 15.0$ TeV.

3 Numerical results

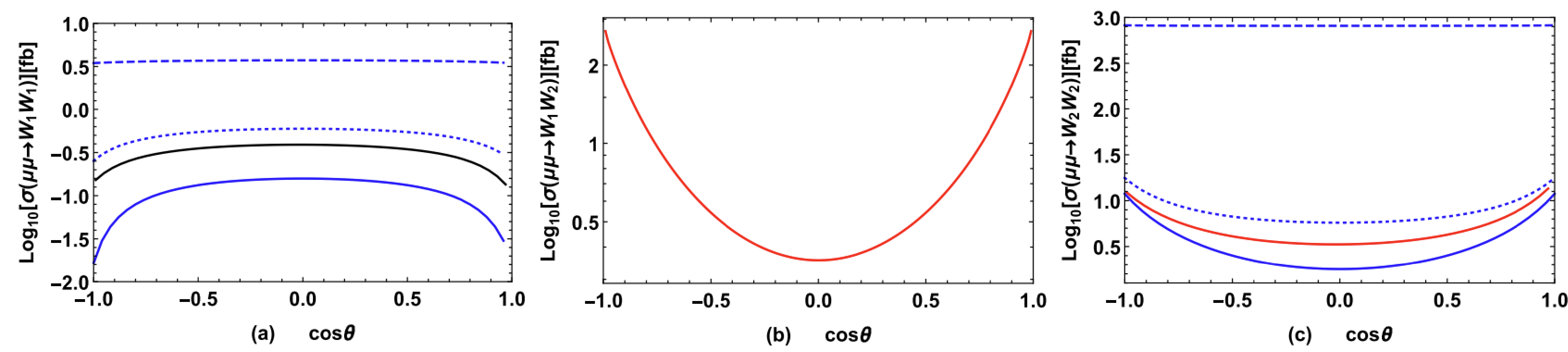

Fig. 8. Taking $M_{N_2} = 2.0\text{TeV}$, $S_\mu^2 = 10^{-4}$, $M_{W_2} = 5.0\ \text{TeV}$, the angle distributions of the LNV processes are plotted. (a): the angle distributions of $\mu^\pm\mu^\pm \to W_1^\pm W_1^\pm$ with $\sqrt{s} = 5.0$ TeV, the black curve denotes the results in **TI-NP**, the blue solid, blue dashed, blue dotted curves denote the results in **TIII-NP** with $Y_{\mu\mu} = 1.0$ for $M_{\Delta_L^{\pm\pm}} = M_{\Delta_R^{\pm\pm}} = 3、5、7$ TeV respectively. (b): the angle distributions of $\mu^\pm\mu^\pm \to W_1^\pm W_2^\pm$ with $\sqrt{s} = 7.0\ \text{TeV}$, where the red curve denotes the results in **TII-NP**. (c): the angle distributions of $\mu^\pm\mu^\pm \to W_2^\pm W_2^\pm$ with $\sqrt{s} = 12.0$ TeV, the red curve denotes the results in **TII-NP**, the blue solid, blue dashed, blue dotted curves denote the results in **TIII-NP** with $Y_{\mu\mu} = 1.0$ for $M_{\Delta_L^{\pm\pm}} = M_{\Delta_R^{\pm\pm}} = 7, 12, 15$ TeV respectively。

4 Summary

1. **The contributions in the three types of NP to the LFV and LNV processes can be identified** by observing the cross sections of these processes at the same-sign muon colliders.

2. The angle distributions of LFV processes are flat in all three types of NP, and **observing the angle distributions of LNV processes** at the same-sign muon colliders **can help to identify the contributions** to these LNV processes come from Majorana neutrinos or doubly charged Higgs.

3. **The high-energy same-sign muon colliders are effective to observe the doubly charged Higgs** through the LFV and LNV processes.

THANKS

Jin-Lei Yang

2024.04.20